

Low frequency fluctuation study using a microwave interferometer and H α line emission measurement systems in the Pilot-PSI device

Cite as: AIP Advances 9, 085225 (2019); <https://doi.org/10.1063/1.5099648>

Submitted: 11 April 2019 . Accepted: 09 August 2019 . Published Online: 26 August 2019

M. Yoshikawa , H. v. d. Meiden, R. AL, J. Vernimmen, J. Kohagura, Y. Shima, M. Sakamoto, and Y. Nakashima

COLLECTIONS

Paper published as part of the special topic on [Chemical Physics](#), [Energy, Fluids and Plasmas](#), [Materials Science](#) and [Mathematical Physics](#)



View Online



Export Citation



CrossMark

ARTICLES YOU MAY BE INTERESTED IN

[Investigating the effect of different impurities on plasma detachment in linear plasma machine Magnum-PSI](#)

Physics of Plasmas **26**, 102502 (2019); <https://doi.org/10.1063/1.5120180>

[Direct numerical simulation of a supersonic turbulent boundary layer subject to adverse pressure gradient induced by external successive compression waves](#)

AIP Advances **9**, 085215 (2019); <https://doi.org/10.1063/1.5112040>

[Simulation of the two-dimensional Rayleigh-Taylor instability problem by using diffuse-interface model](#)

AIP Advances **9**, 085312 (2019); <https://doi.org/10.1063/1.5100791>



NEW: TOPIC ALERTS

Explore the latest discoveries in your field of research

[SIGN UP TODAY!](#)

Low frequency fluctuation study using a microwave interferometer and H α line emission measurement systems in the Pilot-PSI device

Cite as: AIP Advances 9, 085225 (2019); doi: 10.1063/1.5099648

Submitted: 11 April 2019 • Accepted: 9 August 2019 •

Published Online: 26 August 2019



M. Yoshikawa,^{1,a)}  H. v. d. Meiden,² R. AL,² J. Vernimmen,² J. Kohagura,¹ Y. Shima,¹ M. Sakamoto,¹ and Y. Nakashima¹

AFFILIATIONS

¹Plasma Research Center, University of Tsukuba, 1-1-1 Tennodai, Tsukuba, Ibaraki 305-8577, Japan

²FOM Institute DIFFER–Dutch Institute for Fundamental Energy Research, Partner in the Trilateral Euregio Cluster, 5612 AJ Eindhoven, The Netherlands

^{a)}Corresponding author: M. Yoshikawa e-mail: yosikawa@prc.tsukuba.ac.jp

ABSTRACT

A frequency multiplied microwave interferometer, a H α line emission measurement system, and a high speed camera system were installed on the Pilot-PSI device for low frequency fluctuation study in the detached plasma condition. The two dimensional H α line emission and its fluctuation were monitored with a fast visible camera with H α filter. The coherent low frequency fluctuations of frequency of approximately 13 kHz were measured by all measurement systems. The stronger fluctuation intensities were observed in the downstream of the ionization front region in the detached plasma condition. Moreover, we show the clear difference between the strong fluctuation regions of the electron line density and H α line emission for the first time. This means that the fluctuations of H α line emissions was caused by not only electrons but also by hydrogen ions.

© 2019 Author(s). All article content, except where otherwise noted, is licensed under a Creative Commons Attribution (CC BY) license (<http://creativecommons.org/licenses/by/4.0/>). <https://doi.org/10.1063/1.5099648>

I. INTRODUCTION

Detached plasma production is one of the most important objects for DEMO reactor for decreasing the heat flux to the divertor plate. The detached plasma conditions are successfully produced in the linear plasma devices with optimization of background gas pressures and plasma source parameters.^{1–16} In the detached plasma condition, the coherent fluctuation with the frequency of $E \times B$ drift is observed in many linear plasma devices.^{10–16} The fluctuation study in the divertor plasma devices are carried out to understand the intermittent convective plasma transport across magnetic field lines, for example, nonlinear processes related to instabilities and thought to be responsible for the particle and energy loss to the wall, are commonly referred to as blobs.^{1–5} Detailed studies of blobs and density fluctuations have been performed mainly by using Langmuir probes with measuring the ion saturation current and floating potential.^{1–5} In the divertor simulation linear plasma devices, electron density fluctuations have not been clearly observed. Microwave

interferometry systems are employed to measure the electron line integrated density and its fluctuations in divertor relevant plasmas.^{11–14} In order to study the mechanisms of the fluctuations in the detached plasma condition, we installed the frequency multiplied microwave interferometer system, the H α emission detector, and a high speed camera system to study fluctuations in the Pilot-PSI device. Pilot-PSI is a magnetized linear plasma device designed for investigations of plasma-surface interactions at ITER relevant parameters.^{16–21} The objective of the study is to know the fluctuation characteristics in the detached plasma condition. The strong fluctuations were observed around the recombination front region where the strong gradients of plasma parameter existed in the detached plasma conditions.^{11–15} In the other researches except for pilot-PSI, there were no measurements of microwave interferometer system and H α line emission system, simultaneously, while the Langmuir probe and the microwave interferometer system were mainly used for fluctuation study. They have an advantage to measure the plasma without disturbances. In this research, we simultaneously use the

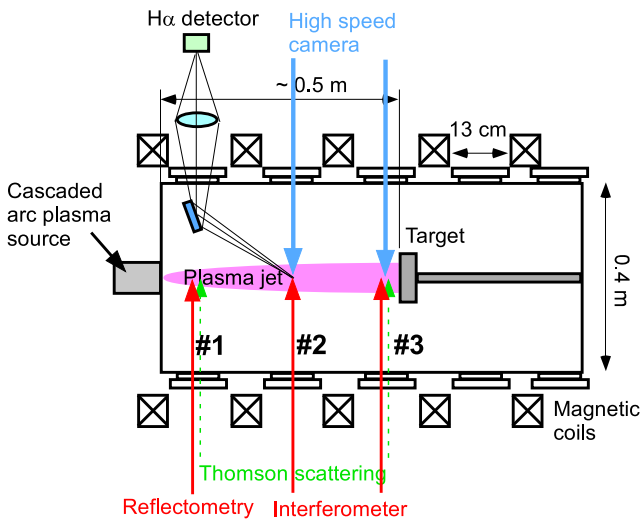


FIG. 1. Schematic diagram of the Pilot-PSI device and diagnostic systems.

microwave interferometer system and Ha line emission measurement systems to study fluctuation characteristics in the detached plasma of Pilot-PSI device. The fluctuation frequency of approximately 13 kHz which caused by $E \times B$ drift was observed and the two dimensional fluctuation characteristics of Ha line emissions show the radial and axial fluctuations in the detached plasma conditions for the first time. We found that strong fluctuation region of the Ha line emission was observed at the upstream from the strong fluctuation region of the electron line density for the first time.

II. EXPERIMENTAL APPARATUS

Schematic view of Pilot-PSI is shown in Fig. 1. It consists of a 1 m long and 40 cm diameter stainless steel vacuum vessel

placed inside five magnetic fields coils. The plasma is produced by a cascaded arc discharge operating in various gases ($z = 0$ mm).¹⁶ An axial magnetic field of up to 1.6 T confines the plasma on the axis of the vessel in the form of a 0.5 m long beam of about 1-2 cm in diameter. In this study the arc was operated in hydrogen at a gas flow of 3.5 standard liter per minute (slm; 1 slm = 4.5×10^{20} particles/s). A discharge current (I) and a magnetic field strength (B) were changed from 80 to 100 A and from 0.4 to 1.6 T shot-by-shot, respectively. The pressure in the vacuum vessel during arc operation is usually kept at a value of 1 – 10 Pa. To facilitate the plasma detachment, we have varied the background pressure in the range of 5.5 – 18.0 Pa by the means of changing the pumping speed. The electron density and temperature near the target is less than $1 \times 10^{11} \text{ cm}^{-3}$ and 0.1 eV, respectively. In this plasma condition, the detached plasma is produced.

The frequency multiplied microwave interferometer system (Fig. 2), which was constructed in GAMMA 10,^{11–14,22} was located at either about 290 mm downstream of the source nozzle ($z = 290$ mm, port #2) or at a distance of about 30 mm in front of the target surface ($z = 550$ mm, port #3). It is a heterodyne interferometer system equipped with a 17.5-GHz phase locked dielectric resonator oscillator, a 37.5-MHz temperature-compensated crystal oscillator, as well as frequency multipliers for obtaining 70 GHz probing beam and reference beam. The interferometer design achieves a frequency stable interferometer system. Horn antennas are set perpendicularly to the plasma beam. The cut off plasma density of the system is $6 \times 10^{13} \text{ cm}^{-3}$. Spatial resolution of the interferometer system is about 3 cm. Phase detection signals are recorded by an oscilloscope (Tektronix, DPO4034) with sampling rate of 1 MSa/s.

Molecular Activated Recombination (MAR) and ion electron recombination are efficient production channels for excited neutrals.²⁰ Ha line emission fluctuation could depend on both the electron and hydrogen ion fluctuations. To investigate this, a Ha line emission detector of photodiode (Thorlabs, SM1PD1A) and a fast visible camera (Phantom V12.1, 55009 fps, 256×256 pixels, and 12 bit) equipped with an Ha band pass filter were used. The Ha line emission detector was set at the upstream port ($z = 50$ mm,

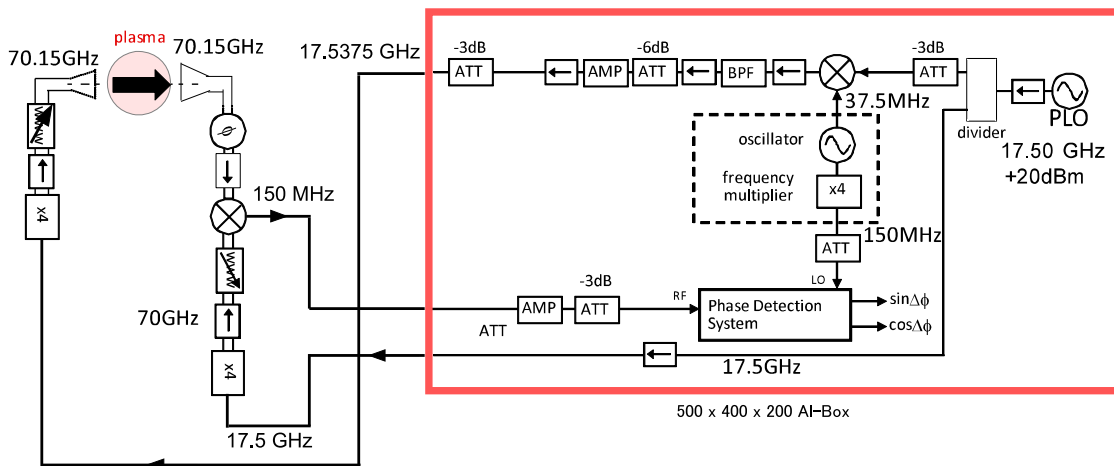


FIG. 2. The frequency multiplied microwave interferometer system.

port #1) with the mirror to view the same observation cord with the interferometer system and the output signal is observed by the same oscilloscope as the interferometer system. The fast camera system was located at the same observation port as the interferometer system after removing the interferometer.

Thomson scattering system was also installed at two ports ($z = 50$ mm at port #1 and 500 mm at port #3) for measuring electron temperature and density radial profiles. It can measure them in a 1 mm spatial resolution and 10 Hz time resolution. Details of the system were shown in elsewhere.²¹

Target plate is divided in three circle plates to investigate the radial potential profile and is set at $z = 550$ mm. The output signal of the core plate potential is measured by the same oscilloscope as the interferometer system.

III. FLUCTUATION MEASUREMENTS

Hydrogen plasma was produced with changing the magnetic field and discharge current of $B = 0.4, 0.8, 1.0, 1.2,$ and 1.6 T, and $I = 80, 100, 110,$ and 120 A, respectively, shot-by-shot. The plasma duration was 7 s. In the typical Pilot-PSI plasma, increase of the magnetic field strength shows the increase of electron density, and increase of the discharge current also shows the increase of electron density. The electron temperature slightly decreases along with the increase of the magnetic field strength and discharge current. Figure 3 shows the electron line density, H α line emission, and target plate voltage measured by the interferometer system and H α line emission detector, and target plate, respectively, measured at port #2 with magnetic field of $B = 0.8$ T and discharge current of $I = 80$ A. The line integrated density is about 2×10^{13} cm⁻². The averaged electron density

is about 1×10^{13} cm⁻³. Electron density and temperature measured by the Thomson scattering system are about 4×10^{14} cm⁻³ and 3 eV at port #1 and less than 1×10^{13} cm⁻³ and less than 0.2 eV at port #3, respectively, which showed that the plasma was in the detached plasma condition. The FFT analysed spectra of the electron line integrated density, H α line emission, and the target plate potential are shown in Fig. 4(a), 4(b), and 4(c), respectively. They show the same strong coherent low frequency fluctuation of about 13 kHz and the higher harmonics. In Fig. 5(a), 5(b), 5(c), and 5(d), we show a fast camera image at $t = 4.0$ s, a two dimensional (2D) image of fluctuation power spectral density (PSD) at fluctuation frequency of 13 kHz, a phase angle 2D image, and the power spectrum of the fluctuation at the pixel position of $(X, Z) = (150, 250)$ on $B = 0.8$ T and $I = 100$ A, respectively. The 2D images of PSD and phase angle are calculated by the FFT analysis to the time evolution of each 5×5 pixels averaged intensity of H α emission. The left and right side represent the downstream and upstream of the plasma, respectively. The stronger fluctuation intensity was observed in the upstream in Fig. 5(b). A pixel size is about 0.4 mm in the image. The core plasma diameter at the upstream is about 100 pixels and 4 cm. The low frequency fluctuation of frequency of 13 kHz was clearly observed by the fast camera. The fluctuation peak frequency remains at about 13 kHz during the magnetic field strength scan from $B = 0.8$ T to 1.6 T.

IV. DISCUSSION

We show the electron line densities (red circles) and their fluctuation intensities (green diamonds) which are the peak PSD of FFT analysed line density fluctuation at frequency of 12-14 kHz, and H α line emission intensities and their fluctuation intensities which

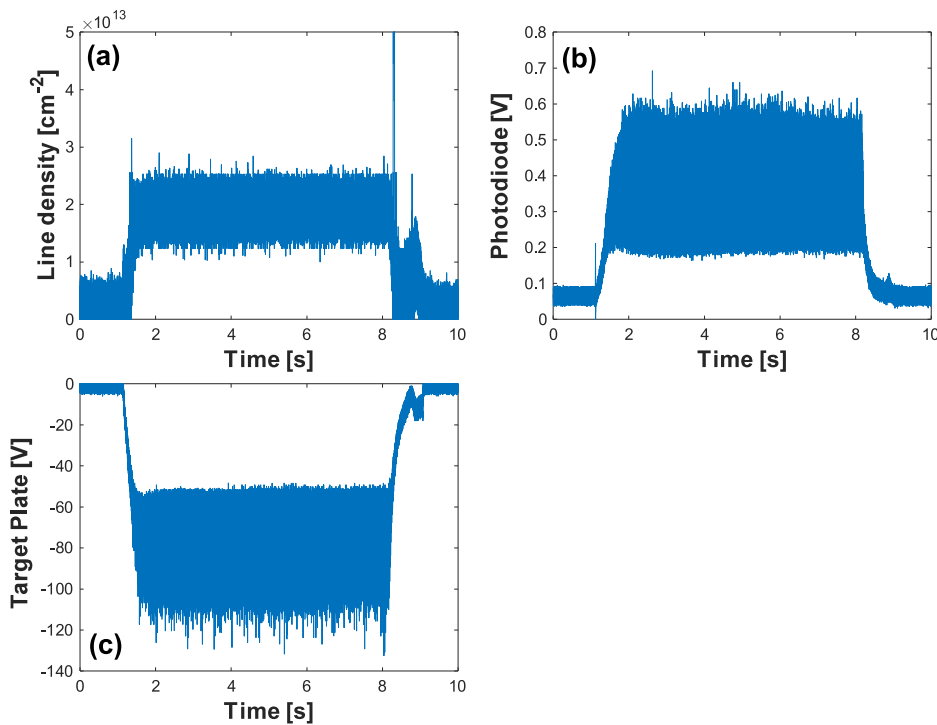


FIG. 3. (a) Line density, (b) H α line emission and (c) target plate voltage on the plasma at the conditions of $B = 0.8$ T and $I = 80$ A.

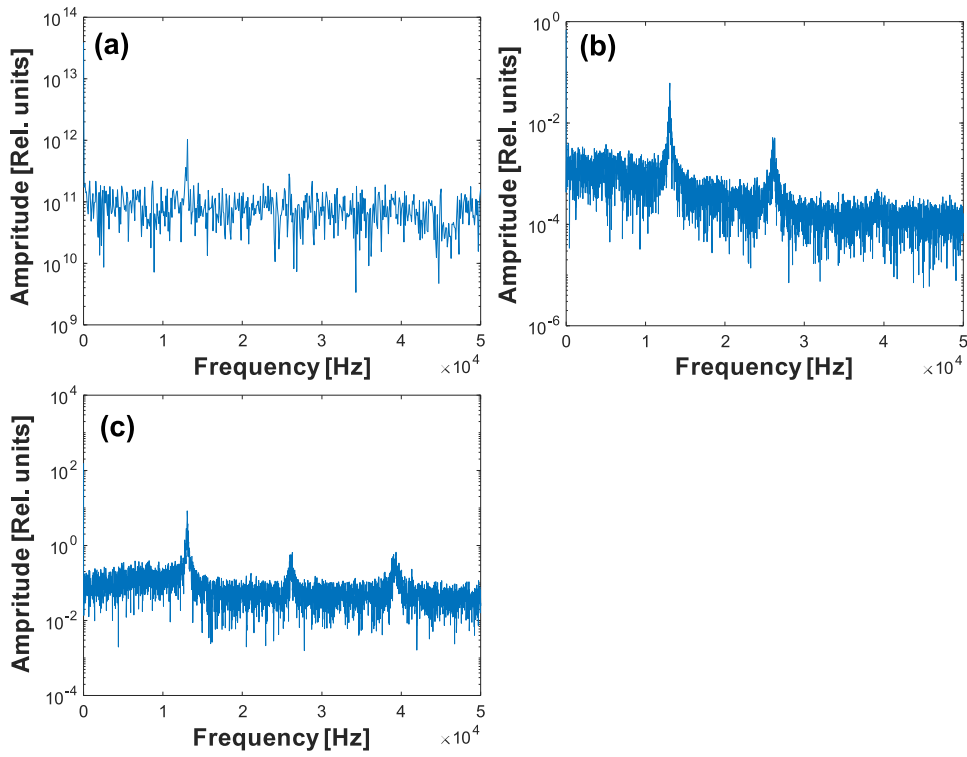


FIG. 4. (a), (b) and (c) show the FFT analysed spectra of the line integrated density, H α emission detector, and the target plate potential, respectively.

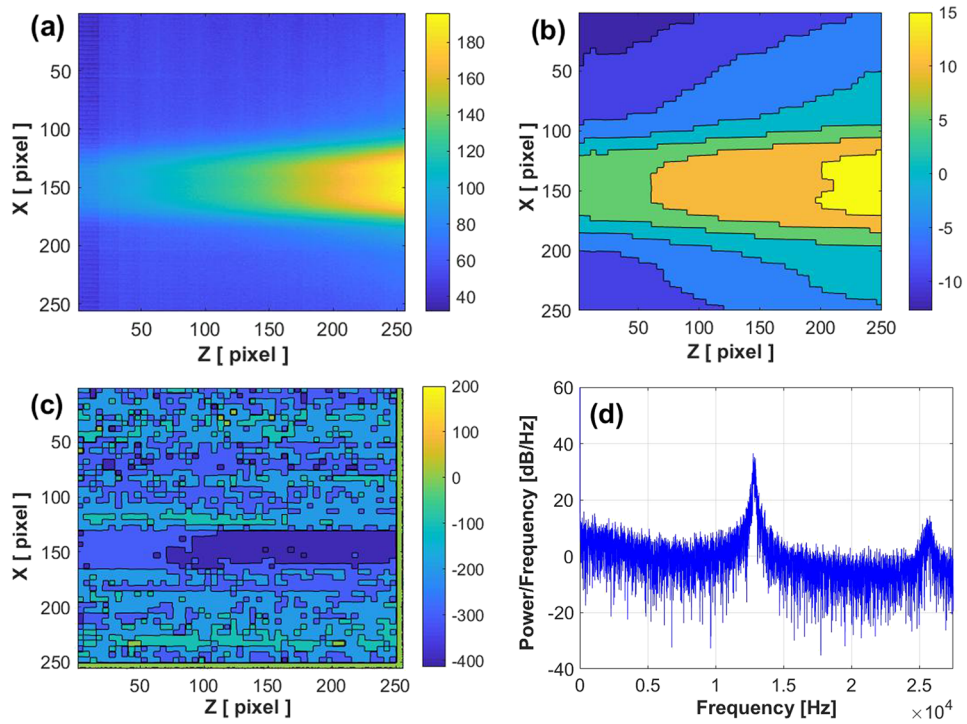


FIG. 5. (a), (b), (c) and (d) show the H α emission of 2D image, 2D image of PSD at the frequency of 13 kHz, 2D image of the phase angle of fluctuation at frequency of 13 kHz, and power spectrum of the fluctuation at pixel position of (X, Z) = (150, 250) on B = 0.8 T and I = 100 A, respectively.

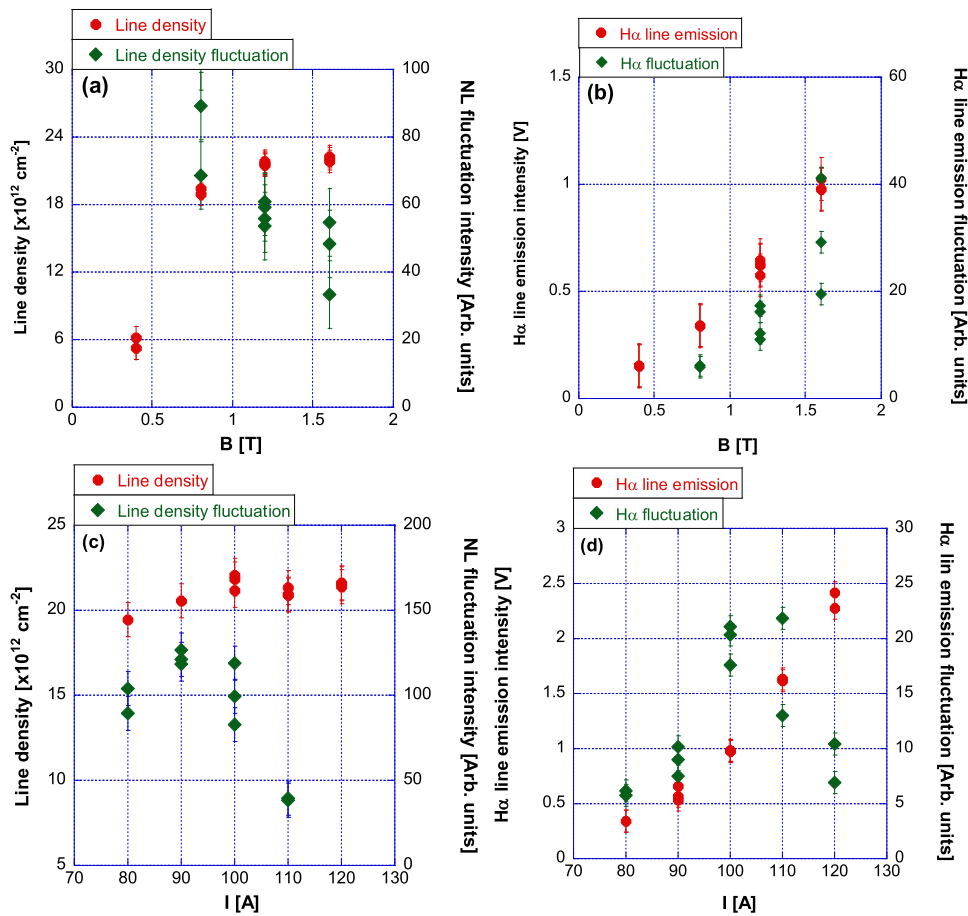


FIG. 6. (a) and (b) show the line densities and their fluctuation intensities and H α line emission intensities and their fluctuation intensities against magnetic field strength at $I = 80$ A, respectively. (c) and (d) show the line densities and their fluctuation intensities and H α line emission intensities and their fluctuation intensities against discharge current at $B = 0.8$ T, respectively.

are the same as the line density fluctuation intensities, against magnetic field strength at discharge current of $I = 80$ A in Fig. 6(a) and 6(b), respectively, and Fig. 6(c) and 6(d) show that against discharge current at the magnetic field strength of $B = 0.8$ T, respectively. There was no coherent fluctuation at the magnetic field strength of $B = 0.4$ T in all measurements. At the magnetic field strength of $B = 0.4$ T, the plasma density and target plate potential were too low to measure the fluctuation. In Fig. 7, we show the H α emission 2D images, (a) and (c), and 2D images of PSD, (b) and (d), at $B = 1.2$ T and $I = 100$ A, and at $B = 0.8$ T and $I = 110$ A, respectively. As increasing of the magnetic field strength and discharge current, the strong H α line emission region expanded to the target plate direction and strong fluctuation region also expanded. It means that the detached region near the target plate decreases and the fluctuated region moves to the downstream. The line density and H α line emission intensity increase along with increase of the magnetic field strength. The increasing rate of line density was almost saturated at the magnetic field strength of $B = 1.6$ T. The fluctuation strengths of line density and H α line emission against the magnetic field strengths were not the same. One of the reason of this difference is from the difference of line of sight of the measurements between the microwave interferometer and the H α line emission measurement system. However, the H α emission of 2D images show the same behavior as the H α line emission measurement system. In the H α line emission, the

strong emission intensity region was in the upstream of the high electron density region. In Fig. 6(c) and 6(d), there are peaks in the fluctuation intensities of the line density and H α emission against the discharge current at 90 A and 110 A, respectively. The discharge currents for maximum fluctuation intensities of the electron line density and H α line emission are not the same. This represents that the H α line emission fluctuation was not the only effects of electron density. In this plasma condition, the plasma was in the detached plasma condition and the main H α emissions were caused by the electron-ion recombination (EIR) and MAR. Then the H α line emission fluctuation was caused by electron and ion fluctuation. The strong fluctuation region moves along with the increment of magnetic field strength and discharge current. The strong fluctuation was observed at decreasing region of the axial electron density profile which moves to the downstream along with increase of magnetic field strength and discharge current. While increasing the magnetic field strength and discharge current, the electron line density was saturated. It represents the decrease of the electron density increase and the decreased electrons recombined with the ions at the observing region. Then the H α emission intensity continued to increase and line density saturated. The maximum fluctuation intensity of line density was observed at the discharge current $I = 90$ A and that of H α line emission was at $I = 110$ A. This means that the strong fluctuation region of H α line emission is observed at upstream of that of line density.

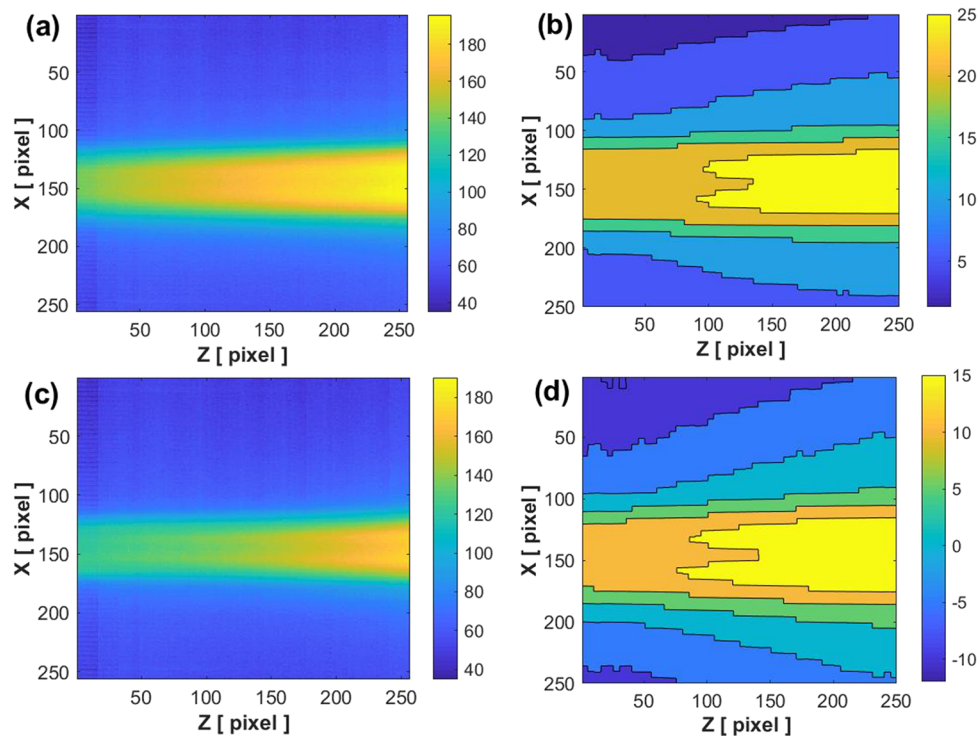


FIG. 7. (a), (c) and (b), (d) show the H α emission of 2D images and 2D image of PSD at B = 1.2 T and I = 100 A, and at B = 0.8 T and I = 120 A, respectively.

In Fig. 5(b), the fluctuation intensity is stronger at the plasma core region and upstream of the plasma. The fluctuation is clearly observed outside of the main plasma column compared to the H α line emission image shown in Fig. 5(a). The 2D phase angle image shows that the phase angle of the fluctuation is maintained axially from the upstream to downstream and the radially rotating characteristics were observed. In Fig. 8, we show the phase angle averaged over axial direction radial dependence. The phase angle difference at the frequency of 13 kHz between the upper region of X = 150 and the

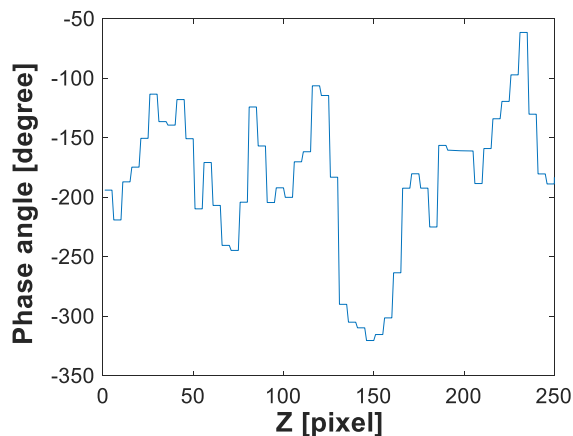


FIG. 8. Phase angle averaged over Z direction radial dependence.

lower region of X = 200 in Fig. 8 is approximately 159° . The observed fluctuation depends on the plasma rotation. Such fluctuation frequency could correspond to the rotation velocity at the plasma edge is about 2×10^3 m/s. We calculate the electric field of approximately 30 V/cm by the target plate potential of 60 V and plasma radius of 2 cm. The $E \times B$ drift rotation velocity of $v_r = E/B$ is 4×10^3 m/s. The obtained rotation velocities by the rotation frequency and the $E \times B$ drift rotation are comparable.

We have found that four independent diagnostics measure the same coherent low frequency fluctuation in Pilot-PSI. In these plasma condition which we measured the low frequency fluctuation, the MAR and ion electron recombination (IER) are dominant effect to produce the excited neutrals.²⁰ The fluctuations were mainly produced by the rotating electrons. However, ions must be also rotating in the frequency of $E \times B$ drift rotation and affect the H α emission fluctuation. In this experiment, we could not identify the efficiency of the ion rotation to the fluctuation.

As increasing the magnetic field strength, the electron density increased and as increasing the discharge current, the electron density mainly increased. The electron temperature slightly decreased along with the electron density increase. In Fig. 9, we show the electron density and temperature against the discharge current at the magnetic field strength of 1.2 T measured by the Thomson scattering system settled at #1 port. Unfortunately, we could not obtain the electron density and temperature dependences against the magnetic field strength. However, we show those dependences against the magnetic field strength at discharge current of 200 A on the another experiments in Fig. 9(b). It was hard to measure the electron

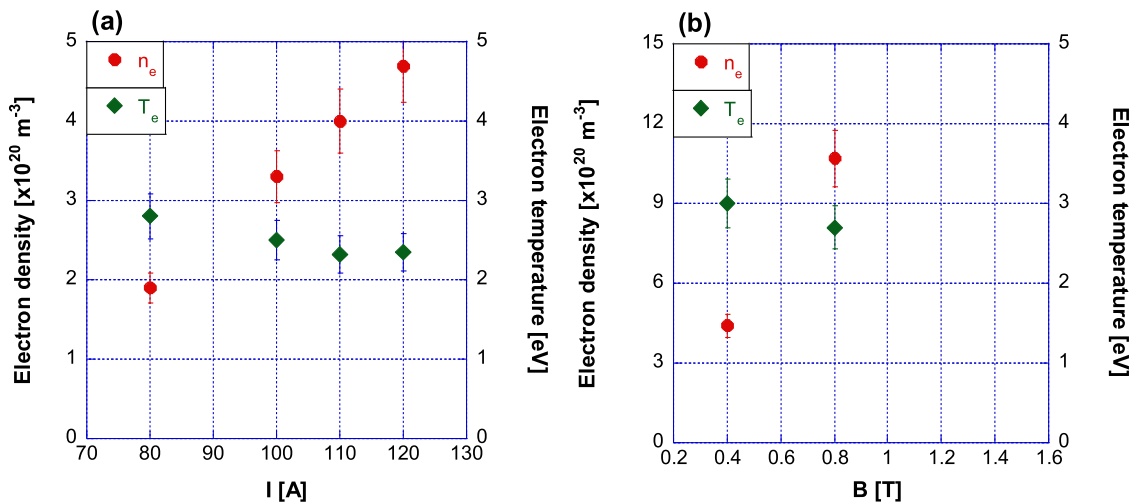


FIG. 9. (a) Shows the electron density and temperature against the discharge current at the magnetic field strength of 1.2 T and (b) shows them against the discharge current of 200 A measured by the Thomson scattering system settled at #1 port.

density and temperature at #3, because of low electron density region of detached plasma condition. The strong fluctuations were observed around the magnetic field strength of 1.0 T and the plasma discharge current of 100 A. The strong fluctuation region moves to the downstream with increase of the magnetic field strength and discharge current. Then the fluctuation intensities of the electron densities and H α line emissions were changed at the observation region with changing magnetic field strength and plasma discharge current. In the detached plasma condition, the electron density and temperature decreased along the magnetic field to the target plate.¹ In front of the ionization front region where is upstream of the recombination front region, the electron density and H α line emission intensity are larger and higher than that in the downstream plasma. The strong fluctuation intensities were observed in the detached plasma condition and it seems to be in the ionization region. Moreover, the strong fluctuation region of H α line emission was in the upstream of that of the electron line density. The fluctuations of H α line emissions were caused by not only the electrons by also by the hydrogen ions.

V. CONCLUSION

We measured the coherent low frequency fluctuations by using the microwave interferometer system and H α emission measurements by photodiode and high speed camera systems without plasma disturbance, and the target plate, simultaneously, for the first time, in the Pilot-PSI device. The coherent fluctuation frequency of approximately 13 kHz which caused by $E \times B$ drift was obtained in all measurement systems. The strong fluctuation intensity was observed in the downstream of the ionization front region and that is in front of the recombination front. The strong fluctuation region of the H α line emission was observed at the upstream from the strong fluctuation region of the electron line density for the first time. This means

that the fluctuations of H α line emissions were caused by both the electron and hydrogen ions.

ACKNOWLEDGMENTS

This work is partly supported by the PWI international collaboration program and performed with the support and under the auspices of the NIFS Collaboration Research program (NIFS14KUGM086).

REFERENCES

- N. Ohno *et al.*, *Nucl. Fusion* **41**, 309 (2001).
- H. Tanaka *et al.*, *Contrib. Plasma Phys.* **50**, 256 (2010).
- H. Tanaka *et al.*, *Nucl. Fusion* **49**, 065017 (2009).
- H. Tanaka *et al.*, *Phys. Plasmas* **17**, 102509 (2010).
- H. Tanaka *et al.*, *Contrib. Plasma Phys.* **52**, 424 (2012).
- S. Kado *et al.*, *J. Nucl. Mater.* **313-316**, 754 (2003).
- A. Okamoto *et al.*, *Rev. Sci. Instrum.* **76**, 116106 (2005).
- E. M. Hollmann *et al.*, *Phys. Plasmas* **20**, 093303 (2013).
- Y. Nakashima *et al.*, *Nucl. Fusion* **57**, 116033 (2017).
- K. Okazaki *et al.*, *Rev. Sci. Instrum.* **83**, 023502 (2012).
- M. Yoshikawa *et al.*, *Plasma Fusion Res.* **10**, 1202088 (2015).
- K. Takeyama *et al.*, *Plasma Fusion Res.* **12**, 1202007 (2017).
- H. Tanaka *et al.*, *Plasma Phys. Control. Fusion* **60**, 075013 (2018).
- H. Natsume *et al.*, *AIP Advances* **9**, 015016 (2019).
- Y. Hayashi *et al.*, *Nucl. Fusion* **56**, 126006 (2016).
- B. D. Groot *et al.*, *Fusion Eng. Design* **82**, 1861 (2007).
- J. Westerhout *et al.*, *Phys. Scr.* **T128**, 18 (2007).
- W. Vijvers *et al.*, *Phys. Plasmas* **15**, 093507 (2008).
- G. van Rooij *et al.*, *Appl. Phys. Lett.* **90**, 121501 (2007).
- A. Shumack *et al.*, *Phys. Rev. E* **78**, 046405 (2008).
- H. V. D. Meiden *et al.*, *Rev. Sci. Instrum.* **79**, 013505 (2008).
- J. Kohagura *et al.*, *Trans. Fusion Sci. Technol.* **63**, 176 (2013).